EUROPEAN LABORATORY FOR PARTICLE PHYSICS

CERN-PPE/96-137
9th October 1996

A Measurement of the Average Bottom Hadron Lifetime

The OPAL Collaboration

Abstract

The average b hadron lifetime, τ_b, has been measured using approximately 3.5 million hadronic events collected with the OPAL detector at LEP between 1991 and 1994. A lifetime tag based on a neural network algorithm was used to select $Z^0 \to b\bar{b}$ events. A secondary vertex reconstructed on the opposite side from the b-tag was used to measure the b hadron decay length. This was combined with an estimate of the b hadron momentum, allowing the b hadron decay time to be evaluated. The lifetime,

$$\tau_b = 1.611 \pm 0.010\,(\text{stat}) \pm 0.027\,(\text{syst})\,\text{ps},$$

was extracted from a fit involving the distribution of the 95 620 decay times reconstructed in the data and the corresponding distribution in Monte Carlo.

(Submitted to Z. Phys. C)

The OPAL Collaboration

K. Ackerstaff[8], G. Alexander[23], J. Allison[16], N. Altekamp[5], K. Ametewee[25], K.J. Anderson[9], S. Anderson[12], S. Arcelli[2], S. Asai[24], D. Axen[29], G. Azuelos[18,a], A.H. Ball[17], E. Barberio[8], R.J. Barlow[16], R. Bartoldus[3], J.R. Batley[5], J. Bechtluft[14], C. Beeston[16], T. Behnke[8], A.N. Bell[1], K.W. Bell[20], G. Bella[23], S. Bentvelsen[8], P. Berlich[10], S. Bethke[14], O. Biebel[14], V. Blobel[27], I.J. Bloodworth[1], J.E. Bloomer[1], M. Bobinski[10], P. Bock[11], H.M. Bosch[11], M. Boutemeur[34], B.T. Bouwens[12], S. Braibant[12], R.M. Brown[20], H.J. Burckhart[8], C. Burgard[8], R. Bürgin[10], P. Capiluppi[2], R.K. Carnegie[6], A.A. Carter[13], J.R. Carter[5], C.Y. Chang[17], D.G. Charlton[1,b], D. Chrisman[4], P.E.L. Clarke[15], I. Cohen[23], J.E. Conboy[15], O.C. Cooke[16], M. Cuffiani[2], S. Dado[22], C. Dallapiccola[17], G.M. Dallavalle[2], S. De Jong[12], L.A. del Pozo[8], K. Desch[3], M.S. Dixit[7], E. do Couto e Silva[12], M. Doucet[18], E. Duchovni[26], G. Duckeck[34], I.P. Duerdoth[16], J.E.G. Edwards[16], P.G. Estabrooks[6], H.G. Evans[9], M. Evans[13], F. Fabbri[2], P. Fath[11], F. Fiedler[27], M. Fierro[2], H.M. Fischer[3], R. Folman[26], D.G. Fong[17], M. Foucher[17], A. Fürtjes[8], P. Gagnon[7], A. Gaidot[21], J.W. Gary[4], J. Gascon[18], S.M. Gascon-Shotkin[17], N.I. Geddes[20], C. Geich-Gimbel[3], F.X. Gentit[21], T. Geralis[20], G. Giacomelli[2], P. Giacomelli[4], R. Giacomelli[2], V. Gibson[5], W.R. Gibson[13], D.M. Gingrich[30,a], D. Glenzinski[9], J. Goldberg[22], M.J. Goodrick[5], W. Gorn[4], C. Grandi[2], E. Gross[26], J. Grunhaus[23] M. Gruwé[8], C. Hajdu[32], G.G. Hanson[12], M. Hansroul[8], M. Hapke[13], C.K. Hargrove[7], P.A. Hart[9], C. Hartmann[3], M. Hauschild[8], C.M. Hawkes[5], R. Hawkings[8], R.J. Hemingway[6], M. Herndon[17], G. Herten[10], R.D. Heuer[8], M.D. Hildreth[8], J.C. Hill[5], S.J. Hillier[1], T. Hilse[10], P.R. Hobson[25], R.J. Homer[1], A.K. Honma[28,a], D. Horváth[32,c], R. Howard[29], R.E. Hughes-Jones[16], D.E. Hutchcroft[5], P. Igo-Kemenes[11], D.C. Imrie[25], M.R. Ingram[16], K. Ishii[24], A. Jawahery[17], P.W. Jeffreys[20], H. Jeremie[18], M. Jimack[1], A. Joly[18], C.R. Jones[5], G. Jones[16], M. Jones[6], R.W.L. Jones[8], U. Jost[11], P. Jovanovic[1], T.R. Junk[8], D. Karlen[6], K. Kawagoe[24], T. Kawamoto[24], R.K. Keeler[28], R.G. Kellogg[17], B.W. Kennedy[20], B.J. King[8], J. Kirk[29], S. Kluth[8], T. Kobayashi[24], M. Kobel[10], D.S. Koetke[6], T.P. Kokott[3], M. Kolrep[10], S. Komamiya[24], T. Kress[11], P. Krieger[6], J. von Krogh[11], P. Kyberd[13], G.D. Lafferty[16], H. Lafoux[21], R. Lahmann[17], W.P. Lai[19], D. Lanske[14], J. Lauber[15], S.R. Lautenschlager[31], J.G. Layter[4], D. Lazic[22], A.M. Lee[31], E. Lefebvre[18], D. Lellouch[26], J. Letts[2], L. Levinson[26], C. Lewis[15], S.L. Lloyd[13], F.K. Loebinger[16], G.D. Long[17], M.J. Losty[7], J. Ludwig[10], A. Malik[21], M. Mannelli[8], S. Marcellini[2], C. Markus[3], A.J. Martin[13], J.P. Martin[18], G. Martinez[17], T. Mashimo[24], W. Matthews[25], P. Mättig[3], W.J. McDonald[30], J. McKenna[29], E.A. Mckigney[15], T.J. McMahon[1], A.I. McNab[13], R.A. McPherson[8], F. Meijers[8], S. Menke[3], F.S. Merritt[9], H. Mes[7], J. Meyer[27], A. Michelini[2], G. Mikenberg[26], D.J. Miller[15], R. Mir[26], W. Mohr[10], A. Montanari[2], T. Mori[24], M. Morii[24], U. Müller[3], K. Nagai[26], I. Nakamura[24], H.A. Neal[8], B. Nellen[3], B. Nijjhar[16], R. Nisius[8], S.W. O'Neale[1], F.G. Oakham[7], F. Odorici[2], H.O. Ogren[12], N.J. Oldershaw[16], T. Omori[24], M.J. Oreglia[9], S. Orito[24], J. Pálinkás[33,d], G. Pásztor[32], J.R. Pater[16], G.N. Patrick[20], J. Patt[10], M.J. Pearce[1], S. Petzold[27], P. Pfeifenschneider[14], J.E. Pilcher[9], J. Pinfold[30], D.E. Plane[8], P. Poffenberger[28], B. Poli[2], A. Posthaus[3], H. Przysiezniak[30], D.L. Rees[1], D. Rigby[1], S. Robertson[28], S.A. Robins[13], N. Rodning[30], J.M. Roney[28], A. Rooke[15], E. Ros[8], A.M. Rossi[2], M. Rosvick[28], P. Routenburg[30], Y. Rozen[22], K. Runge[10], O. Runolfsson[8], U. Ruppel[14], D.R. Rust[12], R. Rylko[25], K. Sachs[10], E.K.G. Sarkisyan[23], M. Sasaki[24], C. Sbarra[2], A.D. Schaile[34], O. Schaile[34], F. Scharf[3], P. Scharff-Hansen[8], P. Schenk[27], B. Schmitt[8], S. Schmitt[11], M. Schröder[8], H.C. Schultz-Coulon[10], M. Schulz[8], M. Schumacher[3], P. Schütz[3], W.G. Scott[20], T.G. Shears[16], B.C. Shen[4], C.H. Shepherd-Themistocleous[8], P. Sherwood[15], G.P. Siroli[2], A. Sittler[27], A. Skillman[15], A. Skuja[17], A.M. Smith[8], T.J. Smith[28], G.A. Snow[17], R. Sobie[28], S. Söldner-Rembold[10], R.W. Springer[30], M. Sproston[20], A. Stahl[3], M. Steiert[11], K. Stephens[16], J. Steuerer[27], B. Stockhausen[3], D. Strom[19], F. Strumia[8], P. Szymanski[20], R. Tafirout[18],

S.D. Talbot[1], S. Tanaka[24], P. Taras[18], S. Tarem[22], M. Thiergen[10], M.A. Thomson[8], E. von Törne[3], S. Towers[6], I. Trigger[18], T. Tsukamoto[24], E. Tsur[23], A.S. Turcot[9], M.F. Turner-Watson[8], P. Utzat[11], R. Van Kooten[12], G. Vasseur[21], M. Verzocchi[10], P. Vikas[18], M. Vincter[28], E.H. Vokurka[16], F. Wäckerle[10], A. Wagner[27], C.P. Ward[5], D.R. Ward[5], J.J. Ward[15], P.M. Watkins[1], A.T. Watson[1], N.K. Watson[7], P.S. Wells[8], N. Wermes[3], J.S. White[28], B. Wilkens[10], G.W. Wilson[27], J.A. Wilson[1], G. Wolf[26], S. Wotton[5], T.R. Wyatt[16], S. Yamashita[24], G. Yekutieli[26], V. Zacek[18],

[1]School of Physics and Space Research, University of Birmingham, Birmingham B15 2TT, UK
[2]Dipartimento di Fisica dell' Università di Bologna and INFN, I-40126 Bologna, Italy
[3]Physikalisches Institut, Universität Bonn, D-53115 Bonn, Germany
[4]Department of Physics, University of California, Riverside CA 92521, USA
[5]Cavendish Laboratory, Cambridge CB3 0HE, UK
[6] Ottawa-Carleton Institute for Physics, Department of Physics, Carleton University, Ottawa, Ontario K1S 5B6, Canada
[7]Centre for Research in Particle Physics, Carleton University, Ottawa, Ontario K1S 5B6, Canada
[8]CERN, European Organisation for Particle Physics, CH-1211 Geneva 23, Switzerland
[9]Enrico Fermi Institute and Department of Physics, University of Chicago, Chicago IL 60637, USA
[10]Fakultät für Physik, Albert Ludwigs Universität, D-79104 Freiburg, Germany
[11]Physikalisches Institut, Universität Heidelberg, D-69120 Heidelberg, Germany
[12]Indiana University, Department of Physics, Swain Hall West 117, Bloomington IN 47405, USA
[13]Queen Mary and Westfield College, University of London, London E1 4NS, UK
[14]Technische Hochschule Aachen, III Physikalisches Institut, Sommerfeldstrasse 26-28, D-52056 Aachen, Germany
[15]University College London, London WC1E 6BT, UK
[16]Department of Physics, Schuster Laboratory, The University, Manchester M13 9PL, UK
[17]Department of Physics, University of Maryland, College Park, MD 20742, USA
[18]Laboratoire de Physique Nucléaire, Université de Montréal, Montréal, Quebec H3C 3J7, Canada
[19]University of Oregon, Department of Physics, Eugene OR 97403, USA
[20]Rutherford Appleton Laboratory, Chilton, Didcot, Oxfordshire OX11 0QX, UK
[21]CEA, DAPNIA/SPP, CE-Saclay, F-91191 Gif-sur-Yvette, France
[22]Department of Physics, Technion-Israel Institute of Technology, Haifa 32000, Israel
[23]Department of Physics and Astronomy, Tel Aviv University, Tel Aviv 69978, Israel
[24]International Centre for Elementary Particle Physics and Department of Physics, University of Tokyo, Tokyo 113, and Kobe University, Kobe 657, Japan
[25]Brunel University, Uxbridge, Middlesex UB8 3PH, UK
[26]Particle Physics Department, Weizmann Institute of Science, Rehovot 76100, Israel
[27]Universität Hamburg/DESY, II Institut für Experimental Physik, Notkestrasse 85, D-22607 Hamburg, Germany
[28]University of Victoria, Department of Physics, P O Box 3055, Victoria BC V8W 3P6, Canada
[29]University of British Columbia, Department of Physics, Vancouver BC V6T 1Z1, Canada
[30]University of Alberta, Department of Physics, Edmonton AB T6G 2J1, Canada
[31]Duke University, Dept of Physics, Durham, NC 27708-0305, USA
[32]Research Institute for Particle and Nuclear Physics, H-1525 Budapest, P O Box 49, Hungary
[33]Institute of Nuclear Research, H-4001 Debrecen, P O Box 51, Hungary
[34]Ludwigs-Maximilians-Universität München, Sektion Physik, Am Coulombwall 1, D-85748 Garching, Germany

[a] and at TRIUMF, Vancouver, Canada V6T 2A3
[b] and Royal Society University Research Fellow
[c] and Institute of Nuclear Research, Debrecen, Hungary
[d] and Department of Experimental Physics, Lajos Kossuth University, Debrecen, Hungary

1 Introduction

Two main techniques are used to measure the average b hadron lifetime, $\tau_{\rm b}$, at LEP energies. The first and most widely adopted method uses maximum likelihood fits to the distribution of the impact parameters of leptons from semileptonic b hadron decays [1, 2], where the impact parameter is the distance of closest approach of the lepton to the $\rm e^+e^-$ collision point. Previous measurements of $\tau_{\rm b}$ by the OPAL collaboration used this technique. The most recent result, $\tau_{\rm b} = 1.523 \pm 0.034\,(\rm stat) \pm 0.038\,(\rm syst)$ ps, was measured from data collected between 1990 and 1991 [2]. The second method uses inclusively reconstructed secondary vertices to estimate the decay length of the b hadron [3]. It is interesting to compare results from these two techniques, as the systematic errors are largely uncorrelated. In particular, there is no reliance on the modelling of semileptonic b hadron decays in the second method. This is the method used in the analysis described in this paper.

This paper is organised as follows. A brief description of the OPAL detector is given in section 2. The data samples and selection procedure are presented in section 3. The analysis method is described in section 4 and the procedure used to select $\rm Z^0 \to b\bar{b}$ events is detailed in section 5. Section 6 describes the procedure for reconstructing the b hadron decay time. The fitting techniques used to extract the lifetime are defined in section 7. The results and systematic error studies are detailed in sections 8 and 9, respectively. Finally, the results are summarised and compared to other recent results in section 10.

2 The OPAL Detector

The OPAL detector was used to collect data from decays of the $\rm Z^0$ boson, produced in $\rm e^+e^-$ collisions at the LEP collider at CERN. The OPAL detector is equipped with a central tracking system comprising a silicon microvertex detector, a precision vertex drift chamber, a large volume jet chamber and z-chambers. It is positioned inside a solenoid that provides a uniform magnetic field of 0.435 T. The coil is surrounded by a lead-glass electromagnetic calorimeter with a presampler, a hadron calorimeter and muon chambers. A detailed description of the whole detector can be found elsewhere [4]. The most important component for this analysis is the central tracking system. The jet chamber provides tracking and ionization energy loss ($\rm d$$E$/$\rm d$$x$) measurements [5], and is surrounded by a set of chambers to measure the z-coordinate[a] of tracks as they exit the jet chamber. In 1991, a high precision silicon microvertex detector [6] was installed around the beryllium-composite beam pipe at the interaction point. In 1993, the silicon detector was upgraded [7] to supply additional tracking information in the z-coordinate, but only r-ϕ silicon microvertex detector information is used for the analysis described in this paper. The impact parameter resolution in the x-y plane achieved for 45 GeV[b] tracks in $\rm Z^0 \to \mu^+\mu^-$ events is 18 μm for tracks with associated hits in each of the two layers of the silicon microvertex detector.

3 Data Samples and Selection Procedure

This analysis was performed on approximately 3.5 million hadronic events collected in the vicinity of the $\rm Z^0$ peak between 1991 and 1994 with the silicon microvertex detector operational. Hadronic $\rm Z^0$ decays were selected using criteria described in a previous publication [8], where

[a] In the OPAL right-handed coordinate system the x-axis points towards the centre of the LEP ring, the y-axis points upwards and the z-axis points in the direction of the electron beam. The polar angle θ and the azimuthal angle ϕ are defined with respect to z and x, respectively, while r is the distance from the z-axis.

[b] We use the notation $c = 1$ throughout this paper.

the selection efficiency was measured to be (98.4±0.4)%. The central tracking system and electromagnetic calorimeters were required to have been fully operational when the data were collected.

Monte Carlo hadronic events were generated using the JETSET 7.4 program [9] with parameters tuned to OPAL data [10]. The production rates of b hadrons were in the ratio B^0:B^+:B_s:b baryon = 40:40:12:8, and the lifetimes of B mesons and b baryons were set to 1.6 ps and 1.2 ps, respectively. These lifetimes are consistent with the 1996 PDG averages [11], which give $\tau(B^+) = 1.62 \pm 0.06$ ps, $\tau(B^0) = 1.56 \pm 0.06$ ps, $\tau(B_s) = 1.61^{+0.10}_{-0.09}$ ps and an average b baryon lifetime of 1.14 ± 0.08 ps. The fragmentation function of Peterson *et al.* [12] was used for the b quarks. Two types of Monte Carlo sample are used in this analysis. In the default sample the fragmentation parameter ε_b was set to 0.004, which corresponds to a mean scaled energy of $\langle x_E \rangle$=0.703 for the weakly-decaying b hadron. In the 'modified fragmentation' sample, ε_b was set to 0.006, resulting in $\langle x_E \rangle$=0.680. Recent measurements [13] give $\langle x_E \rangle$=0.701±0.008, indicating that the default sample provides better modelling of the b fragmentation properties.

To simulate the detector response, the Monte Carlo event samples were processed with the detector simulation program [14]. Comparisons between data and Monte Carlo revealed significant discrepancies in the tails of track impact parameter distributions. For the default samples, an *ad hoc* smearing procedure was applied to the impact parameter and ϕ measurements in order to bring these distributions into agreement. In this procedure, for 8.5% of the tracks (chosen at random) the impact parameters were smeared by 1.5 σ, and a further 1% of tracks had their impact parameters smeared by 8.5 σ, where σ represents the estimated uncertainty on the impact parameter from the fitted track parameters. Figure 1 shows the distributions of d_0 and d_0/σ_{d_0}, the impact parameter significance, observed for tracks in the data, where d_0 is the impact parameter in the x-y plane with respect to the primary vertex, and σ_{d_0} denotes the error on d_0. For these distributions only tracks with momenta larger than 0.5 GeV and with $|d_0| < 0.3$ cm were selected. The sign of d_0 is chosen to be positive if the point of closest approach of the track to the primary vertex, in the x-y plane, is in the same hemisphere as the jet containing the track, otherwise it is negative. The tuning was performed for tracks with negative values of d_0, since the negative side of the distribution is sensitive to resolution effects, and is relatively insensitive to lifetime contributions. Also shown in the figure are the corresponding distributions for Monte Carlo, with and without the smearing. The agreement between data and Monte Carlo is clearly improved by the smearing. Event samples without this *ad hoc* smearing were also used, and are referred to as 'unsmeared' in this paper.

4 Analysis Method

Each event was divided into two hemispheres using the thrust axis of the event. The thrust axis was required to satisfy $|\cos\theta| < 0.75$, otherwise the event was rejected. Hemispheres were tagged as containing candidate b hadrons ('b-tagged') using secondary vertices reconstructed with the algorithm described in [15]. Properties of such secondary vertices were used as inputs to a neural network algorithm that was trained to select $Z^0 \to b\bar{b}$ events [16]. According to Monte Carlo studies, this procedure results in a sample that is approximately 96% pure in $Z^0 \to b\bar{b}$ events for an efficiency per hemisphere of about 17%.

Charged tracks and electromagnetic clusters not associated with a charged track were resolved into jets using a 'cone' algorithm [17]. The size of the cone was chosen to include nearly all the decay products of a b hadron into one jet. The jets also include particles produced in the fragmentation process which originate from the e^+e^- collision point. Only events with exactly two jets were used in this analysis to reduce the number of events where both b quarks lie in the same hemisphere due to the emission of an energetic gluon.

The hemisphere opposite a b-tag was searched for secondary vertices using a vertex finding

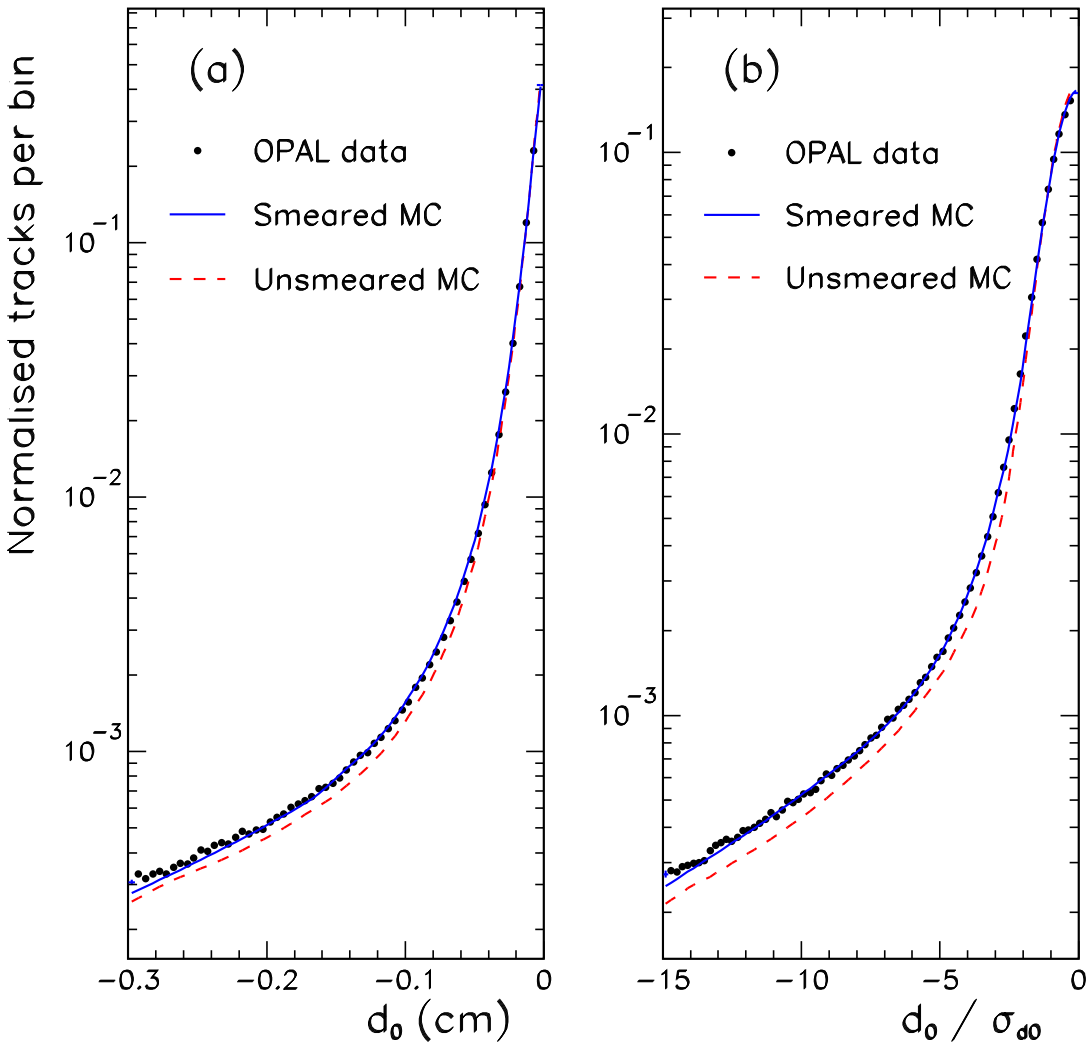

Figure 1: *The distributions of (a) track impact parameters and (b) impact parameter significances in data compared to Monte Carlo with and without the smearing described in the text.*

algorithm (described in section 6) which was more suited to measuring accurate decay lengths, rather than just providing a b-tag. The primary event vertex was reconstructed using the charged tracks in the event, constrained by the average position and spread of the e^+e^- collision point. The decay length between the primary event vertex and the secondary vertex (on the opposite side of the event from the b-tag) was converted into a decay time using an estimate of the b hadron momentum. The average b hadron lifetime was extracted from a fit involving the distribution of reconstructed decay times in both data and Monte Carlo.

5 Selecting $Z^0 \to b\bar{b}$ Events and Purity Determination

Candidate $Z^0 \to b\bar{b}$ events were selected by using seven properties of secondary vertices reconstructed using the algorithm described in [15] as inputs to a neural network algorithm [16]. The most important inputs are the decay length, its uncertainty, the vertex multiplicity and track

impact parameter significances. The neural network allows a very high purity sample of $Z^0 \to b\bar{b}$ events to be isolated.

The double tagging technique described in [18] was used to determine the b purity of the tagged jet in the data events satisfying the two jet requirement. This avoids unnecessary dependence on Monte Carlo modelling. The number of singly tagged hemispheres, N_v, and the number of events with two tagged hemispheres, N_{vv}, in a sample of $N_{\rm had}$ hadronic events can be expressed as :

$$N_v = 2\left(\epsilon_{\rm b}\,\frac{\Gamma_{\rm b\bar{b}}}{\Gamma_{\rm had}} + \epsilon_{\rm c}\,\frac{\Gamma_{\rm c\bar{c}}}{\Gamma_{\rm had}} + \epsilon_{\rm uds}\,\frac{\Gamma_{\rm u\bar{u}}+\Gamma_{\rm d\bar{d}}+\Gamma_{\rm s\bar{s}}}{\Gamma_{\rm had}}\right) N_{\rm had}\ , \tag{1}$$

$$N_{vv} = \left(C_{\rm b}\epsilon_{\rm b}^2\,\frac{\Gamma_{\rm b\bar{b}}}{\Gamma_{\rm had}} + \epsilon_{\rm c}^2\,\frac{\Gamma_{\rm c\bar{c}}}{\Gamma_{\rm had}} + \epsilon_{\rm uds}^2\,\frac{\Gamma_{\rm u\bar{u}}+\Gamma_{\rm d\bar{d}}+\Gamma_{\rm s\bar{s}}}{\Gamma_{\rm had}}\right) N_{\rm had}. \tag{2}$$

The partial widths for Z^0 decays to $q\bar{q}$ relative to all hadronic final states are denoted by $\Gamma_{q\bar{q}}/\Gamma_{\rm had}$, and Standard Model values were used for these ratios, neglecting the contribution from photon exchange. The hemispheric tagging efficiencies for $b\bar{b}$, $c\bar{c}$ and lighter quark events are denoted by $\epsilon_{\rm b}$, $\epsilon_{\rm c}$ and $\epsilon_{\rm uds}$, respectively. The values of $\epsilon_{\rm b}$ and $\epsilon_{\rm c}$ were extracted from the data by solving equations 1 and 2 simultaneously, while $\epsilon_{\rm uds}$ was obtained from Monte Carlo. The coefficient $C_{\rm b}$ describes the efficiency correlation between hemispheres in a $b\bar{b}$ event. This is needed because the tagging probabilities for the two hemispheres are not just correlated through the flavour of the initial quark pair. This coefficient is only evaluated for $b\bar{b}$ events, which dominate the double tagged sample. The numerical value of $C_{\rm b}$ differs from unity for three main reasons : (i) the reconstructed position of the primary vertex and its uncertainty are common to both hemispheres; (ii) gluon emission produces a correlation between the b and $\bar{\rm b}$ hadron momenta, and the emission of an energetic gluon can also cause both the b and $\bar{\rm b}$ quarks to fall into the same hemisphere; (iii) the b and $\bar{\rm b}$ hadrons are usually produced back-to-back, so geometrical correlations will therefore be present if the tagging efficiency is not uniform over the geometrical acceptance of the detector. The relationship

$$C_{\rm b} = \frac{\epsilon_{\rm b}^{vv}}{(\epsilon_{\rm b})^2}, \tag{3}$$

was used to evaluate $C_{\rm b}$, where $\epsilon_{\rm b}^{vv}$ is the double tagging efficiency for $b\bar{b}$ events, evaluated from Monte Carlo. The b purity, $P_{\rm b}$, can be determined using the relationship

$$P_{\rm b} = \frac{2\,\epsilon_{\rm b} N_{\rm had}}{N_v} \cdot \frac{\Gamma_{\rm b\bar{b}}}{\Gamma_{\rm had}}\ . \tag{4}$$

Values of $C_{\rm b}$=(0.970±0.007) and $\epsilon_{\rm uds}$=(0.058±0.002)% were determined from the default Monte Carlo sample. The quoted errors are statistical. The estimated systematic error on $C_{\rm b}$ is ±0.004, based on studies of data and Monte Carlo [19]. The true value of the b purity in the Monte Carlo was $P_{\rm b} = 95.8\%$. The true levels of the c and uds contamination were 3.1% and 1.1%, respectively. The values of $C_{\rm b}$ and $\epsilon_{\rm uds}$ were used to determine $P_{\rm b} = (94.6 \pm 0.5)\%$, where the uncertainty includes the full error on $C_{\rm b}$.

6 Reconstructing the Decay Time

In order to determine the decay time, an estimate of both the decay length, L, and the energy, $E_{\rm b}$, of the candidate b hadron are needed. These are discussed below.

6.1 Decay Length Reconstruction

The hemisphere opposite a b-tag was searched for secondary vertices. The vertex finding algorithm works in the r-ϕ plane to select tracks and to fit the position of the secondary vertex. The two precisely measured tracks (requiring hits in either the silicon microvertex or vertex drift chambers) with the most significant separation from the primary event vertex were taken as seed tracks. Precisely measured tracks that were at least three standard deviations from the primary vertex were also taken as seeds. Separated vertex candidates were formed by considering all possible pairs of seed tracks to form a vertex nucleus. Other tracks were added to this nucleus vertex provided they matched this vertex better than the primary vertex, and the vertex probability, on including the new track, was greater than 1%. If more than one candidate secondary vertex was found by the algorithm, a single secondary vertex was chosen, based on the number of tracks associated with each vertex and the reconstructed vertex positions. The decay length in the r-ϕ plane was calculated for each vertex from a fit to the primary vertex position and the secondary vertex position. The r-ϕ vector momentum sum of the vertex tracks was used to constrain the decay length direction. When fitting the decay length the uncertainty from the primary vertex position is usually negligible, with the dominant errors arising from uncertainties in the track parameters for the secondary vertex and the choice of tracks.

Reconstructed secondary vertices consisting of just two charged tracks were not used in this analysis, as they suffered from large combinatorial backgrounds and therefore behaved in a systematically different manner from other secondary vertex multiplicities. Two-track vertices formed 17% of both the Monte Carlo and data samples.

The following quality requirements were imposed on the secondary vertices used to form the decay length measurement in order to suppress badly reconstructed vertices, where, according to Monte Carlo, the reconstructed decay length is only weakly correlated with the true decay length.

- The transverse miss distance divided by its error is required to be less than three. The transverse miss distance is defined as the distance between the primary and secondary vertices projected onto an axis orthogonal to the summed momentum vector of tracks associated with the secondary vertex. This condition helps to remove secondary vertices formed from random track combinations.

- The decay length error (calculated from the parameters of the tracks making up the secondary vertex) was required to be less than 0.06 cm.

- The invariant mass of the secondary vertex tracks (assuming pion masses) was required to be greater than 0.8 GeV.

- For negative decay lengths, the secondary vertex was rejected if it was more than two standard deviations from the primary vertex. The sign of the decay length was assigned according to the scalar product of the jet direction and the decay length vector.

Table 1 shows the effect of each quality requirement on the efficiency for reconstructing a good secondary vertex from a b hadron decay. The overall efficiency for reconstructing a secondary vertex from b hadron decay that passed all the selection criteria was measured from Monte Carlo to be 66%. The equivalent efficiency for reconstructing a secondary vertex in a non-$b\bar{b}$ event selected by the b-tag was estimated to be 51%.

The decay length, L, was estimated from the reconstructed decay length in the r-ϕ plane, $\ell_{r\phi}$, using

$$L = \frac{\ell_{r\phi}}{\sin\theta} \,, \tag{5}$$

Quality Requirement	Efficiency Loss
Vertex with ≥ 3 tracks	20%
Transverse miss distance significance < 3	7%
Decay length error < 0.06 cm	6%
Vertex mass > 0.8 GeV	4%
Decay length significance > -2	2%
Total	34%

Table 1: *The effect of each quality requirement on the efficiency for identifying secondary vertices from b hadron decays in Monte Carlo.*

where θ is the polar angle of the b hadron, estimated using the jet axis. The uncertainty on $\sin\theta$ is negligible compared to the uncertainty in the two-dimensional decay length and therefore leads to a negligible additional error on the calculation of the three-dimensional decay length. After all the quality requirements, the distribution of $L - L^{'}$, where $L^{'}$ represents the true decay length, had a mean of 0.02 cm and a full width at half maximum (called the central width) of 0.13 cm.

6.2 Boost Determination

The technique used to calculate the boost needed to convert the decay length measurement into a decay time was similar to that used in studies of B meson oscillations [20] and B^{**} production [21] by the OPAL collaboration. The event was treated as a two-body decay of the Z^0, of mass $\mathrm{M} = 91.2\,\mathrm{GeV}$ [11]. The two decay bodies are the b jet, of mass m_{bjet} and momentum p, and the rest of the event, of mass m_{rest} and momentum $-p$. The following relationship, which follows from energy conservation, can be used to estimate the energy of the b jet, E_{bjet} :

$$E_{\mathrm{bjet}} = \frac{\mathrm{M}^2 + m_{\mathrm{bjet}}^2 - m_{\mathrm{rest}}^2}{2\mathrm{M}} \; . \tag{6}$$

The mass of the b jet was assumed to be the mass of the $\mathrm{B}^{\pm}$ and B^0 mesons, 5.28 GeV [11]. Monte Carlo studies showed that the final b hadron decay time estimate is insensitive to the choice of b jet mass. The mass of the rest of the event was calculated from the energy and momentum of charged tracks, assuming pion masses, and unassociated electromagnetic clusters, assuming zero mass, not assigned to the b jet.

If the total fragmentation energy in the b jet is denoted by E_{bfrag}, then the energy of the b hadron, E_{b}, is given by

$$E_{\mathrm{b}} = E_{\mathrm{bjet}} - E_{\mathrm{bfrag}} \; . \tag{7}$$

Charged tracks are classified as coming from b decay or b fragmentation using another neural network algorithm. Unassociated electromagnetic clusters are similarly classified using angular information. The following four parameters were used to classify each track presented to the neural network.

- The d_0 significance with respect to the primary vertex.
- The d_0 significance with respect to the secondary vertex.
- The track momentum.

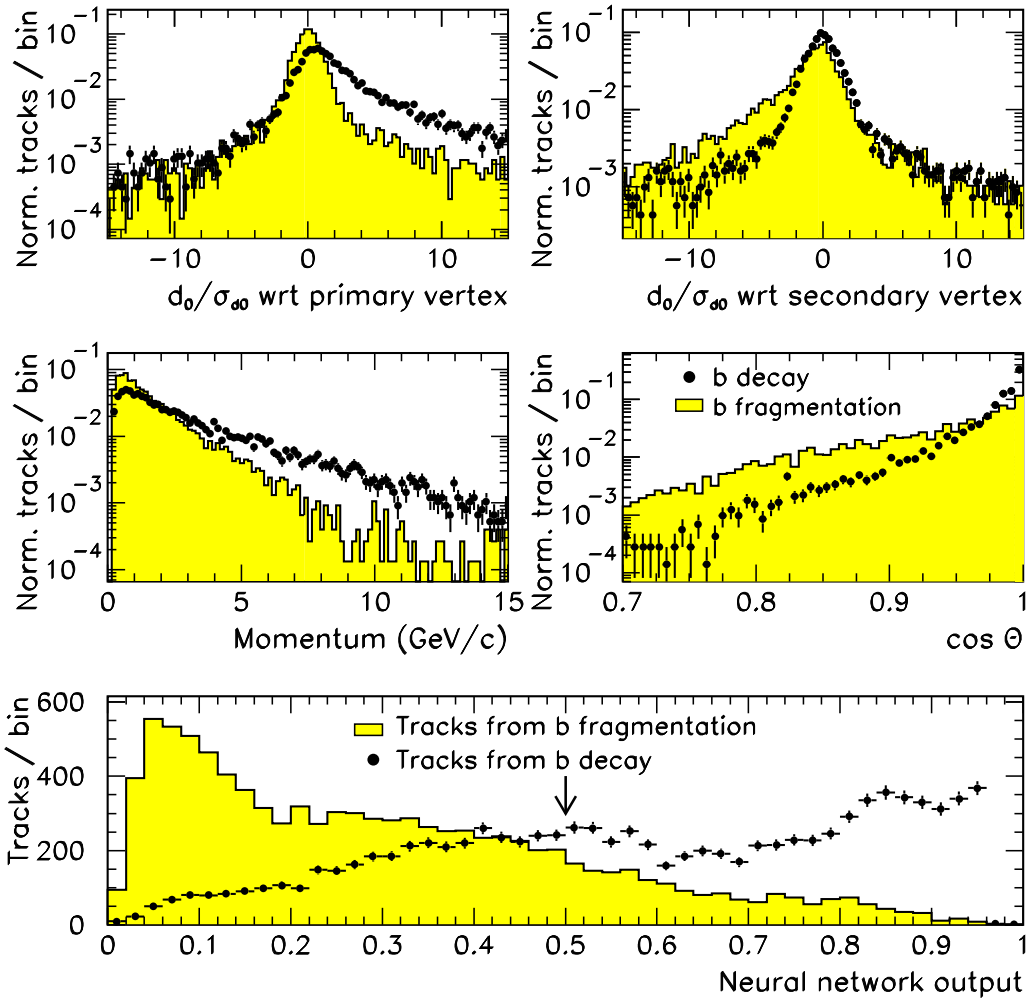

Figure 2: *The upper four plots show the input parameters to the neural network, used to discriminate between tracks from b hadron decay and from b fragmentation. The points represent tracks from b hadron decay and the shaded areas represent tracks from fragmentation in* $Z^0 \to b\bar{b}$ *events. All distributions are normalised to unit area. The output of the neural network for tracks from b hadron decay and fragmentation in* $Z^0 \to b\bar{b}$ *events is also shown. A neural network output below 0.5, indicated by the arrow, was used to select tracks from fragmentation.*

- The value of $\cos\Theta$, where Θ is the angle between the track and the jet axis.

Each of these parameters is shown for tracks from b decay and b fragmentation in figure 2. The neural network was trained on Monte Carlo events to discriminate between tracks from b decay and b fragmentation. The output of the neural network for these two sources of tracks is also shown in figure 2. Monte Carlo studies showed that the best charged b fragmentation energy resolution was obtained when a neural network output of less than 0.5 was used to select tracks from fragmentation.

The neutral fragmentation energy was much harder to identify. Only the angle of the

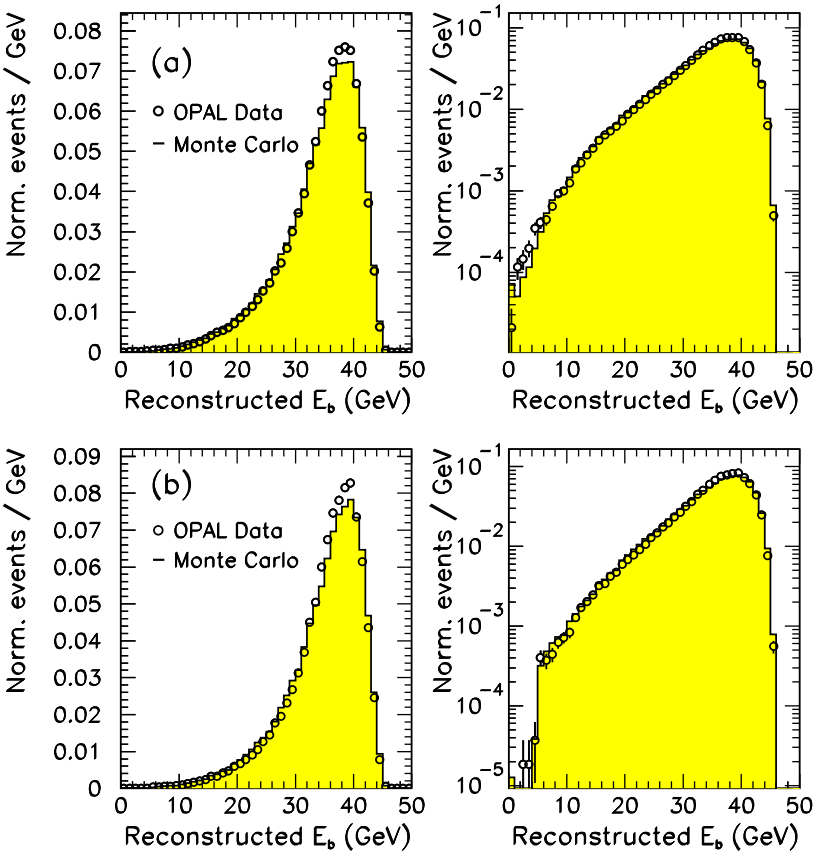

Figure 3: *The reconstructed b hadron energy in Monte Carlo compared to that in data for : (a) all decay times and (b) reconstructed decay times greater than 1 ps, where the energy resolution is improved. The same distributions are shown with a linear scale on the left and a logarithmic scale on the right.*

unassociated electromagnetic cluster relative to the jet axis, $\cos\Theta$, was used. The range of $\cos\Theta$ was split into three : clusters with $\cos\Theta \leq 0.850$ were assigned to b fragmentation; clusters with $\cos\Theta \geq 0.965$ were assumed to originate from b decay; and the energy of clusters in the range $0.965 < \cos\Theta < 0.850$ was shared between the b fragmentation (55%) and b hadron (45%) energy sums. These ranges were tuned to optimise the b hadron energy resolution after the charged fragmentation energy resolution had been optimised.

Using the estimates of the b jet and b fragmentation energies, the b hadron energy was determined and compared to the true value from Monte Carlo. These studies showed that the b hadron energy resolution could be improved when the mass of the rest of the event, $m_{\rm rest}$, was scaled by a factor 87 GeV / $E_{\rm vis}$, where $E_{\rm vis}$ is the total visible energy in the event. The resulting distribution of the b hadron energy resolution has a central width of 8 GeV and is well centred, with a mean of 0.03 GeV. Figure 3 shows the reconstructed b hadron energy in Monte Carlo compared to that in data for all decay times and for reconstructed decay times larger than 1 ps, where the energy resolution is better. The distributions have been normalised to each other and agree well, but small imperfections in the Monte Carlo description of the data are addressed as systematic errors.

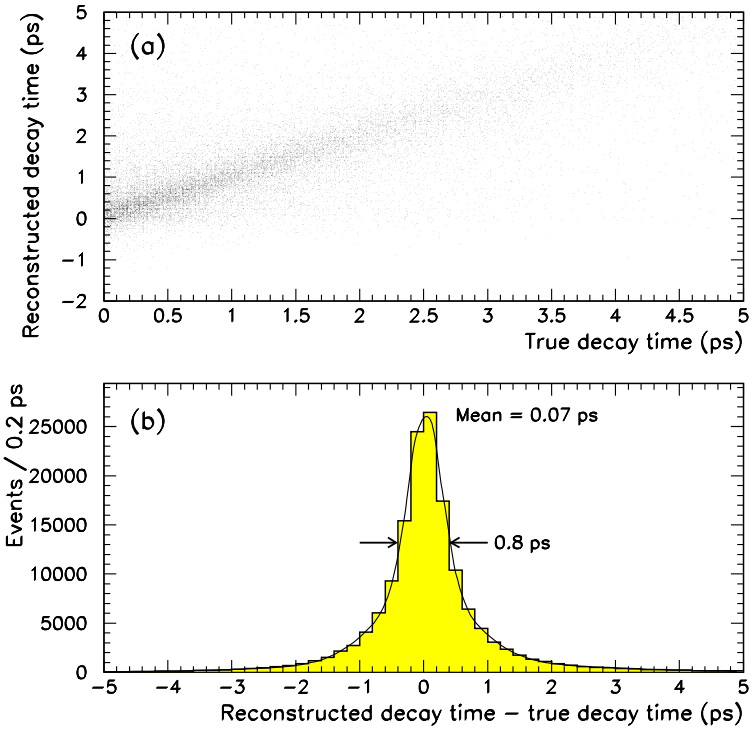

Figure 4: *Plot (a) shows the correlation between reconstructed and true b hadron decay times. Plot (b) shows the decay time resolution. Both plots are from Monte Carlo events.*

6.3 Decay Time

The reconstructed decay time, t, of a b hadron was evaluated by combining the decay length, L, and the reconstructed b hadron energy, $E_{\rm b}$, with the estimated mass of the b hadron, $m_{\rm b}$:

$$\mathrm{t} = \frac{m_{\rm b}\, L}{\sqrt{E_{\rm b}^2 - m_{\rm b}^2}} \,, \tag{8}$$

where $m_{\rm b}$ was chosen to be 5.28 GeV. In cases where $E_{\rm b} < m_{\rm b}$, the event was discarded. Figure 4a shows the correlation between true and reconstructed decay times. The decay time resolution shown in figure 4b has a central width of 0.8 ps and is well centred about zero.

In the next section the technique used to extract the average b hadron lifetime from the reconstructed decay time distribution is discussed.

7 Fitting techniques

A binned maximum likelihood fit may be used to extract $\tau_{\rm b}$ from the distribution of reconstructed decay times. The distribution of reconstructed decay times can be parametrised using : (i) a physics function, which describes the distribution of true decay times as a function of $\tau_{\rm b}$; (ii) a signal resolution function, which describes the distribution of reconstructed decay times, from real b hadron decays, for a given true decay time; and (iii) a background resolution function, which describes the reconstructed decay time distribution of non-$\mathrm{b\bar{b}}$ events. The likelihood

function is described in section 7.1, and the physics function, signal resolution function and background resolution function are described in sections 7.2, 7.3 and 7.4, respectively.

A precise description of the signal resolution function is found to be difficult in this analysis. For this reason, the value of τ_b quoted in this paper is not the one extracted directly from the likelihood fit. The technique used, described in section 7.5, fits the ratio of data and Monte Carlo reconstructed time distributions, where the ratio is parametrised using the likelihood function.

7.1 Likelihood Function

The likelihood function, $\mathcal{L}$, can be defined for N reconstructed decay times, t_i, as

$$\mathcal{L}(\tau_b, \vec{a}) = \prod_{i=1}^{N} \mathbb{P}(t_i; \tau_b, \vec{a}), \tag{9}$$

where

$$\vec{a} = \{\vec{a_p}, \vec{a_s}, \vec{a_b}\}. \tag{10}$$

The normalised probability density function, $\mathbb{P}$, is a function of τ_b, t_i, and the parameters needed to describe the physics, signal resolution and background resolution functions, denoted by $\vec{a_p}$, $\vec{a_s}$ and $\vec{a_b}$, respectively. For a maximum likelihood fit, the estimated value of τ_b is the one that maximises $\mathcal{L}$. The precise form of $\mathbb{P}$ is

$$\mathbb{P}(t; \tau_b, \vec{a}) = \zeta \int_0^\infty \mathcal{P}(t', \tau_b, \vec{a_p}) \mathcal{R}_{sig}(t, t', \vec{a_s})\, dt' + (1-\zeta)\mathcal{R}_{bkgd}(t, \vec{a_b}) \ , \tag{11}$$

where t' represents the true decay time. The physics function is denoted by $\mathcal{P}$ and the signal and background resolution functions by $\mathcal{R}_{sig}$ and $\mathcal{R}_{bkgd}$, respectively. Each of the functions is individually normalised to unity. The parameter ζ describes the amount of signal in the fitted sample. It was derived using the double tagging technique described in section 5 with two corrections. The first correction reduces the background, $(1-\zeta)$, by a factor 0.76 to account for the lower efficiency for the background events to pass the vertex selection cuts, as described in section 6. The second correction, derived from Monte Carlo, reduces ζ by 0.0033 to account for the additional background of events with two b quarks in the same hemisphere due to the emission of an energetic gluon. This additional background is highly suppressed since only events with exactly two jets are used in this analysis. The resulting value is $\zeta = 0.956 \pm 0.006$, including systematic uncertainties of 25% and 50% assigned to the two corrections, respectively.

In the following sections the exact forms of each of the constituent parts of the likelihood function are described in more detail.

7.2 Physics Function

The physics function, which describes the distribution of true decay times as a function of τ_b, is given by

$$\mathcal{P}(t', \tau_b, \vec{a_p}) = \frac{1}{\tau_b} \exp(-t'/\tau_b) \frac{1}{F(t', \vec{a_p})\, \mathcal{N}(\vec{a_p})}, \tag{12}$$

where

$$F(t', \vec{a_p}) = \exp(a + bt') + c, \tag{13}$$

$$\vec{a_p} = \{a, b, c\} \tag{14}$$

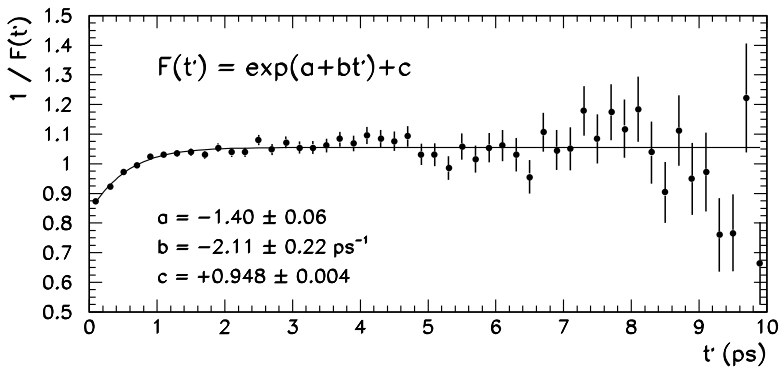

Figure 5: *The bias correction function, 1/F, as a function of true decay time. The bias mainly affects the region $t^{'} < 1$ ps. The fitted parameter values are shown.*

and

$$\mathcal{N}(\vec{a_{\rm p}}) = \int_0^\infty \frac{1}{\tau_{\rm b}} \exp(-t^{'}/\tau_{\rm b}) \, \frac{1}{F(t^{'}, \vec{a_{\rm p}})} \, dt^{'}. \tag{15}$$

As well as a lifetime exponential, the physics function contains a bias correction function, F, which is used to account for the reduced selection efficiency at small true decay times. The bias corrected physics function is normalised by the function $\mathcal{N}$. The integration is performed numerically. The bias arises from two independent sources:

1. Secondary vertex selection. This effect dominates, and shifts the mean of the true decay time distribution by +0.09 ps. The efficiency for detecting a secondary vertex that passes all the quality requirements decreases as the true decay time tends towards zero.

2. Neural network b-tagging. This shifts the mean of the true decay time distribution by –0.03 ps. The reconstructed primary vertex is common to both hemispheres, and events with a b tag tend to have a smaller error on the position of the primary vertex than average. The primary vertex error will be reduced when there are more tracks available for the primary vertex fit. This is more likely when the decay length, and hence the true decay time, is small.

The bias correction function, F, is derived from Monte Carlo from the ratio between the true decay time distributions before and after the application of the b tagging and secondary vertex selection. The distribution of F is well parameterised using the parameter values shown in figure 5. The bias mainly affects the region $t^{'} < 1$ ps.

7.3 Signal Resolution Function

The reconstructed decay time deviates from the true decay time because of imperfect secondary vertex reconstruction and b hadron energy estimation. The relationship between the reconstructed and true decay times is not trivial, and depends on the value of the true decay time. The default Monte Carlo sample was used to parametrise the resolution function, which describes the distribution of reconstructed decay times for a given true decay time.

The shape of the reconstructed decay time distribution for different intervals of true decay time is shown in figure 6. The enhanced number of events around zero in reconstructed decay

time for large true decay times are due to events where the reconstructed secondary vertex consists partially or totally of tracks that originate from the primary vertex. The form of the resolution function is therefore rather complicated as it must account for the peaks in the reconstructed decay time distribution around both zero and the true decay time.

The precise form of the resolution function is

$$\mathcal{R}_{\rm sig}(\mathrm{t},\mathrm{t}^{'},\vec{\mathrm{a}_{\rm s}}) = (1-\mathrm{f}\,\exp\left(-\mathrm{w}\,\mathrm{t}^{'}\right))\Big(\mathrm{g}\,\mathcal{G}_1+(1-\mathrm{g})\,\mathcal{G}_2\Big)+\mathrm{f}\,\exp\left(-\mathrm{w}\,\mathrm{t}^{'}\right)\Big(\mathrm{h}\,\mathcal{G}_3+(1-\mathrm{h})\,\mathcal{G}_4\Big), \tag{16}$$

where $\mathcal{G}_{\rm n}$ represents a unit normalised Gaussian. The parameters f, g and h are restricted to the range $0 < \{\mathrm{f},\,\mathrm{g},\,\mathrm{h}\} < 1$, and describe the relative fraction of each Gaussian such that the resolution function as a whole remains normalised. The Gaussians are described by

$$\underset{\mathrm{n}=1,2}{\mathcal{G}_{\rm n}} = \frac{1}{\sqrt{2\pi}\,\sigma_{\rm n}}\,\exp\left(-\frac{1}{2}\left(\frac{\mathrm{t}-\mathrm{j_n}\mathrm{t}^{'}-\mathrm{k_n}}{\sigma_{\rm n}}\right)^2\right) \tag{17}$$

$$\underset{\mathrm{n}=1,2}{\sigma_{\rm n}} = \alpha_{\rm n}+\beta_{\rm n}\mathrm{t}^{'} \tag{18}$$

and

$$\underset{\mathrm{n}=1,2}{\mathcal{G}_{\mathrm{n}+2}} = \frac{1}{\sqrt{2\pi}\frac{\mathrm{u_n}+\mathrm{v_n}}{2}}\exp\left(-\frac{1}{2}\left(\frac{\mathrm{t}-\varphi_{\rm n}}{\sigma_{\mathrm{n}+2}}\right)^2\right) \tag{19}$$

$$\underset{\mathrm{n}=1,2}{\sigma_{\mathrm{n}+2}} = \begin{cases}\mathrm{u_n} & \text{if } \mathrm{t_i}-\varphi_{\rm n} > 0\\ \mathrm{v_n} & \text{if } \mathrm{t_i}-\varphi_{\rm n} < 0\end{cases} \tag{20}$$

and

$$\vec{\mathrm{a}_{\rm s}} = \{\mathrm{g},\mathrm{h},\mathrm{f},\mathrm{j}_{1,2},\mathrm{k}_{1,2},\alpha_{1,2},\beta_{1,2},\varphi_{1,2},\mathrm{u}_{1,2},\mathrm{v}_{1,2},\mathrm{w}\}\,. \tag{21}$$

Two of the Gaussians, $\mathcal{G}_1$ and $\mathcal{G}_2$, parameterise a non-zero difference between the reconstructed and true decay times and include widths and means that vary linearly with true decay time. The other two Gaussians, $\mathcal{G}_3$ and $\mathcal{G}_4$, are independent of true decay time and have asymmetric widths to account for the difference in tails to negative and positive reconstructed decay times. The term $\exp\left(-\mathrm{w}\,\mathrm{t}^{'}\right)$ reduces the contribution from $\mathcal{G}_{3,4}$ as the true decay time increases. When the true decay time is large there will be many tracks with significant impact parameters and so it is less likely that a secondary vertex will be reconstructed near the primary vertex.

The parametrisation of the reconstructed decay time distributions was performed using a maximum likelihood fitting technique. For example, at $\mathrm{t}^{'} = 1.6$ ps, the value of $\mathrm{f}\exp\left(-\mathrm{w}\,\mathrm{t}^{'}\right)$ was fitted to be 0.19, the values of σ_1 and σ_2 were 0.29 ps and 0.79 ps, respectively, with $\mathrm{g} = 0.52$. Figure 6 shows the reconstructed decay time in several slices of true decay time with the parametrisations from the resolution function overlaid. Imperfections in the parametrisation are visible, but it was found to be difficult to improve the agreement without a considerable increase in the complexity of the parametrisation. These imperfections would be a source of systematic error for the likelihood fit.

7.4 Background Resolution Function

The distribution of reconstructed decay times from background sources (predominantly u,d,s or c quarks on the awayside of a b-tag) is shown in figure 7. A background resolution function, $\mathcal{R}_{\rm bkgd}$,

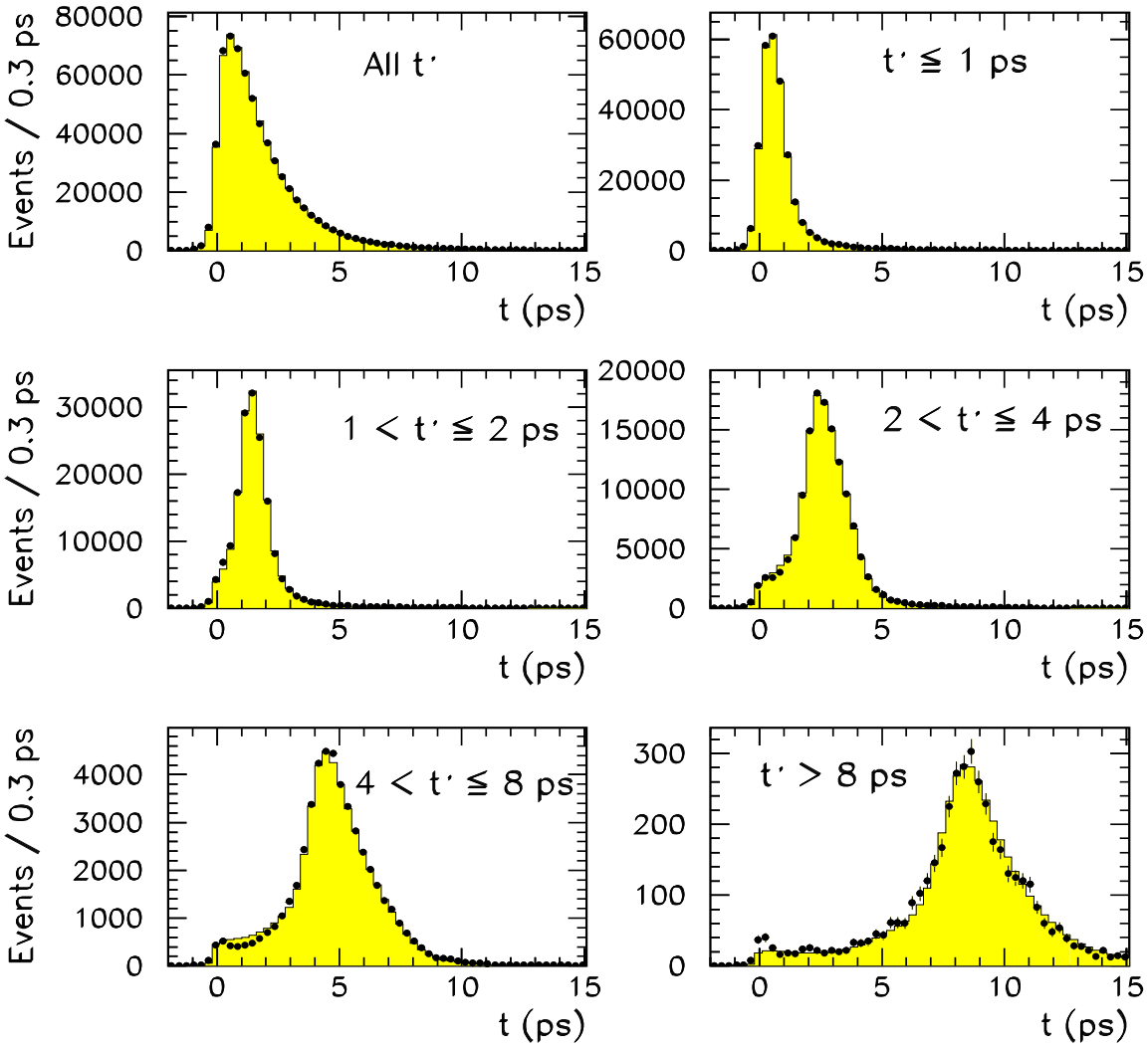

Figure 6: *Distributions of the reconstructed decay time shown for different slices of true decay time for signal events. The points represent the Monte Carlo and the solid histogram is the fit from the signal resolution function.*

consisting of four normalised Gaussians each centred around a unique reconstructed decay time, accurately describes the distribution of reconstructed decay times from background sources :

$$\mathcal{R}_{\rm bkgd}(\mathrm{t}, \vec{\mathrm{a}_{\rm b}}) = \mathrm{q}\Big(\mathrm{r}\,\mathcal{G}'_1 + (1-\mathrm{r})\,\mathcal{G}'_3\Big) + (1-\mathrm{q})\Big(\mathrm{s}\,\mathcal{G}'_2 + (1-\mathrm{s})\,\mathcal{G}'_4\Big), \tag{22}$$

where

$$\underset{\mathrm{n}=1,4}{\mathcal{G}'_{\rm n}} = \frac{1}{\sqrt{2\pi}\,\sigma_{\rm n}}\,\exp\left(-\frac{1}{2}\left(\frac{\mathrm{t}-\chi_{\rm n}}{\sigma_{\rm n}}\right)^2\right), \tag{23}$$

and

$$\vec{\mathrm{a}_{\rm b}} = \{\mathrm{q}, \mathrm{r}, \mathrm{s}, \sigma_{1,4}, \chi_{1,4}\}. \tag{24}$$

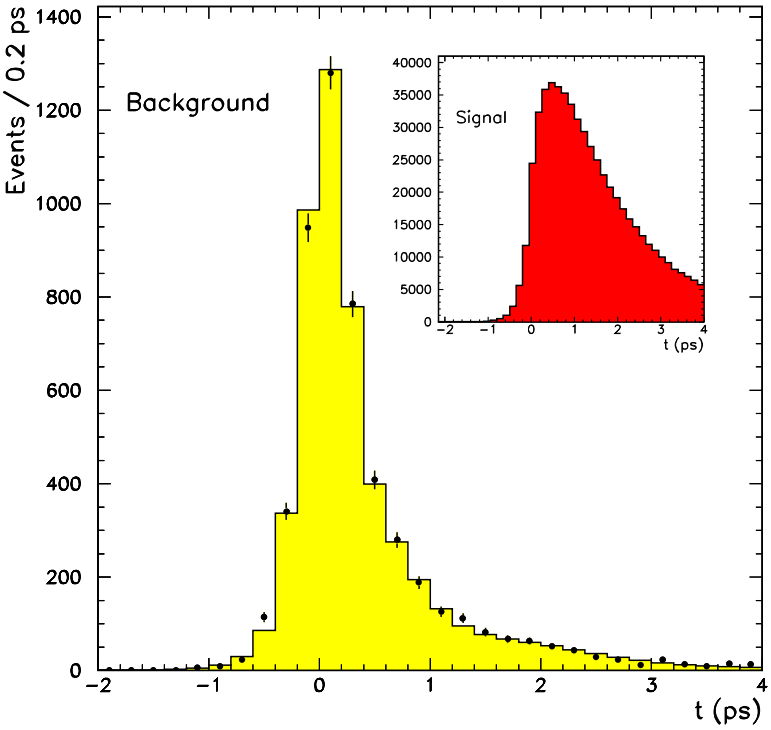

Figure 7: *The reconstructed decay time distribution for background events. The points represent the Monte Carlo and the solid histogram is the fit from the background resolution function. The distribution of reconstructed decay times for signal events is also shown for comparison. The background forms approximately 4% of the total sample.*

Figure 7 shows the parametrisation of the reconstructed time distribution from background sources. The parametrisation agrees well with the simulated data points. The reconstructed time distribution peaks at zero.

7.5 Fit to Data/Monte Carlo

Inaccuracies in the parametrisation of the resolution function represent a problem for a maximum likelihood fit using the likelihood definition as described in the previous sections. This problem may be overcome by dividing the binned reconstructed time distribution observed for data by that seen in Monte Carlo, and by fitting the resulting distribution to the ratio of predicted distributions for data and Monte Carlo as a function of the lifetime assumed for data. The binned predicted distributions, $\mathrm{L}(\mathrm{t};\tau_\mathrm{b},\vec{\mathrm{a}})$, are calculated by integrating $\mathbb{P}(\mathrm{t};\tau_\mathrm{b},\vec{\mathrm{a}})$, defined by equation (11) for the likelihood fit, over the bin size.

In detail, a χ^2 fit was performed between the quantities $\mathbb{S}(\mathrm{t})$ and $\mathbb{L}(\mathrm{t};\tau_\mathrm{b},\vec{\mathrm{a}})$:

$$\mathbb{S}(\mathrm{t}) = \frac{\mathrm{S}_\mathrm{data}(\mathrm{t})}{\mathrm{S}_\mathrm{mc}(\mathrm{t})}, \tag{25}$$

$$\mathbb{L}(\mathrm{t};\tau_\mathrm{b},\vec{\mathrm{a}}) = \frac{\mathrm{L}_\mathrm{data}(\mathrm{t};\tau_\mathrm{b},\vec{\mathrm{a}})}{\mathrm{L}_\mathrm{mc}(\mathrm{t};\tau_\mathrm{mc},\vec{\mathrm{a}}_\mathrm{mc})}; \tag{26}$$

where, $\mathrm{S}_{\mathrm{mc(data)}}(\mathrm{t})$ and $\mathrm{L}_{\mathrm{mc(data)}}(\mathrm{t};\tau,\vec{\mathrm{a}})$ denote the reconstructed decay time distributions and

MC Type	N_{ev}	< -5 ps	>25 ps	ζ	τ_{fit}	τ_{mc}
Default	137 935	0	121	0.964	1.561±0.006	1.571
Unsmeared	103 048	0	86	0.979	1.572±0.007	1.571
Modified fragmentation	70 248	0	68	0.968	1.581±0.009	1.571

Table 2: *The properties of the three Monte Carlo samples used in this analysis. The lifetime fitted from each sample, τ_{fit}, is also shown.*

likelihood predictions from Monte Carlo (data). The principal difference between the parameters for the data, $\vec{a}$, and those for Monte Carlo, $\vec{a}_{mc}$, is the value of ζ, which is based on double tagging. The average b hadron lifetime used for the Monte Carlo was fixed at $\tau_{mc} = 1.571$ ps, the true value for the Monte Carlo, so the only variable in the fit was τ_b. In such a fit, the parametrisation uncertainties should be suppressed by a factor of about $(\tau_b - \tau_{mc})/\tau_{mc}$, where τ_b is the fitted lifetime, and τ_{mc} is the lifetime in the Monte Carlo. It should be stressed that uncertainties in the Monte Carlo simulation of the resolution are not suppressed using this technique, and represent one of the main sources of systematic error for this measurement.

8 Results

In this section, results are presented using the maximum likelihood fit on both Monte Carlo and data. The Monte Carlo results represent a test of the likelihood description. The result of the fit to data/Monte Carlo is also given in this section, and provides the principal result of τ_b for this paper.

Firstly, the likelihood fit for τ_b was tested on Monte Carlo samples, selected in the same way as the data. Three Monte Carlo samples were used: the default sample, a sample without smearing and a sample with modified b fragmentation, as discussed in section 3. The reconstructed decay time distributions were divided into 200 bins from -5 to 25 ps. The numerical integration over true decay time was performed over the range 0 to 20 ps. Table 2 details : the total number of events in the lifetime fit, N_{ev}; the number of events falling outside the binning range; the true proportion of signal events, ζ; the fitted lifetime, τ_{fit}, and the generated lifetime, τ_{mc}. The resolution and bias functions were re-evaluated using the relevant Monte Carlo sample in each test. The fitted lifetime is close to the generated lifetime in each case, indicating that the effect of parametrisation inaccuracies on the fitted lifetime is less than 1% of the lifetime. The parametrised reconstructed decay time distribution for the default Monte Carlo sample is shown in figure 8. The χ^2 between the Monte Carlo and the fitted shape is 500 for 56 degrees of freedom, where the poor agreement reflects the imperfections in the resolution function parametrisation. The b hadron composition of the fitted sample was compared to the original mix in the default Monte Carlo, to check for biases towards a particular b hadron species. The results given in table 3 show there is only a small bias in the fitted sample.

The likelihood fit for τ_b was also performed on the 95 620 reconstructed decay times in the data, using the same binning and integration ranges as described above for the Monte Carlo fits. There was one reconstructed decay time below -5 ps and 76 reconstructed decay times above 25 ps. Using $\zeta = 0.956 \pm 0.006$, as described in section 7, the result of the fit was : $\tau_b = (1.590 \pm 0.007)$ ps, where the error is purely statistical. The reconstructed decay time distribution is shown in figure 9. The χ^2 between the data and the fit is 681 for 57 degrees of freedom.

The χ^2 fit between $\mathbb{S}(t)$ and $\mathbb{L}(t; \tau_b, \vec{a})$, discussed in section 7.5, was first tested on Monte Carlo. By construction the technique gives the correct result for Monte Carlo when the lifetime is

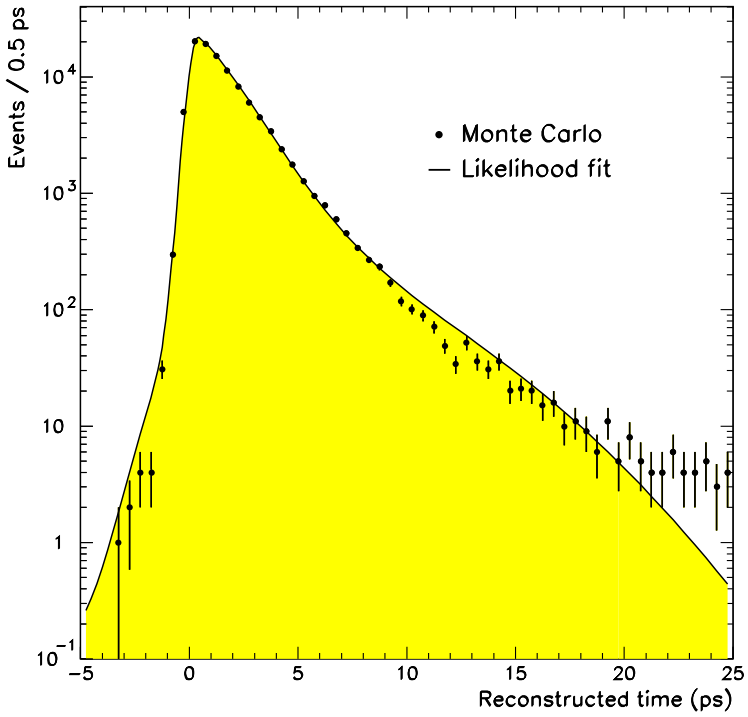

Figure 8: *The reconstructed decay time distribution for Monte Carlo, including backgrounds. The solid line is the result of the lifetime fit.*

b Hadron	Generated Sample	Selected Sample
B meson	92.5%	$(93.3 \pm 0.1)\%$
B^0	43.4%	$(43.1 \pm 0.1)\%$
B^+	43.5%	$(44.4 \pm 0.1)\%$
B_s^0	13.1%	$(12.5 \pm 0.1)\%$
b baryon	7.5%	$(6.7 \pm 0.1)\%$
Λ_b^0	84.5%	$(87.0 \pm 0.3)\%$
Ξ_b^-	7.5%	$(6.4 \pm 0.2)\%$
Ξ_b^0	8.0%	$(6.6 \pm 0.4)\%$

Table 3: *The composition of the b hadron sample in Monte Carlo. The generated and selected sample compositions are shown. The charge conjugate states are included in these numbers.*

left unchanged. To make a non-trivial test, the average lifetime in the Monte Carlo was changed from 1.571 ps to 1.500 ps by rejecting some of the events. The χ^2 fit was then performed, with $\mathbb{S}(t) =$ Monte Carlo($\tau = 1.5$ ps)/Monte Carlo($\tau = 1.571$ ps). For calculation of the ratios, the proper time distributions were binned between -5 and 20 ps, with a minimum of 500 events per bin for the numerator of $\mathbb{S}(t)$. Events with times larger than 20 ps were not used for this fit. The fitted result was $\tau = 1.5003 \pm 0.0081$ ps, where the error ignores the strong correlation between the two Monte Carlo samples. Taking into account the correlation, the error would be

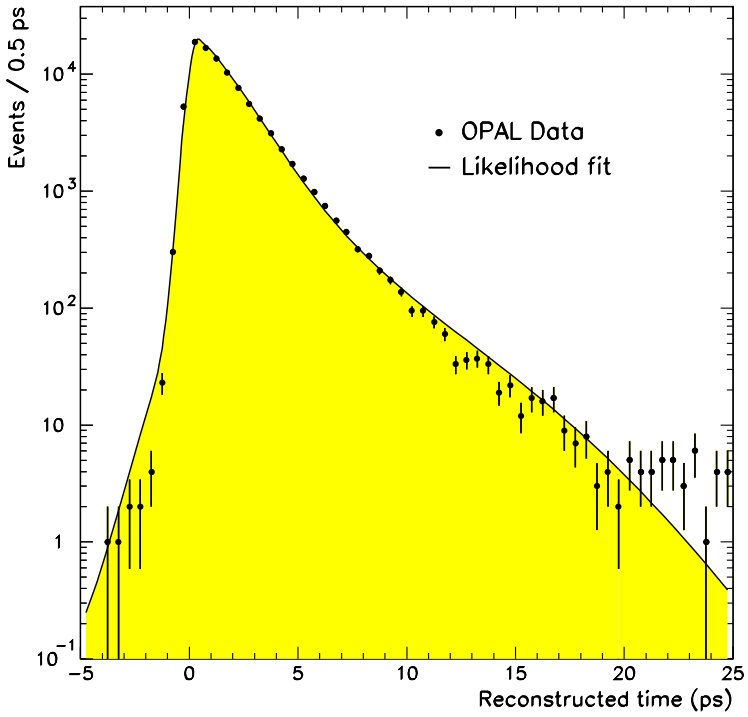

Figure 9: *The reconstructed decay time distribution in data. The solid line is the result of the lifetime fit.*

approximately 0.0017 ps.

Finally, the χ^2 fit between $\mathbb{S}(t)$ and $\mathbb{L}(t;\tau_b,\vec{a})$ was performed for data/Monte Carlo, using the binning strategy described in the previous paragraph, giving

$$\tau_b = (1.597 \pm 0.010)\,\text{ps}, \tag{27}$$

with $\chi^2 = 28.6$ for 17 degrees of freedom. The discrepancies are concentrated in the region $t < 1$ ps, where systematic effects due to background and the bias function are significant. The distribution of $\mathbb{S}(t)$ is shown in figure 10 together with the prediction, $\mathbb{L}(t;\tau_b,\vec{a})$. The agreement is much improved over that seen in figures 8 and 9. The value from this fit is used to derive the final result, after corrections described in the next section.

9 Studies of Systematic Errors

Systematic errors may arise from imperfections in the modelling of b fragmentation and the simulation of the lifetime bias and impact parameter resolution in Monte Carlo. The resolution function is also affected by uncertainties in the production rates of the different charm hadrons in b decays. Further uncertainties follow from the knowledge of the background, and from uncertainties in the alignment of the silicon detector. The systematic errors are summarised in table 4.

Firstly, uncertainties in the Monte Carlo b fragmentation modelling were studied. Such uncertainties predominantly affect the b hadron energy estimate and therefore the parametrisation of the resolution function. Figure 3 shows that the reconstructed b hadron energy in Monte Carlo and data agree well. As a first check, the reconstructed b energy distribution in Monte

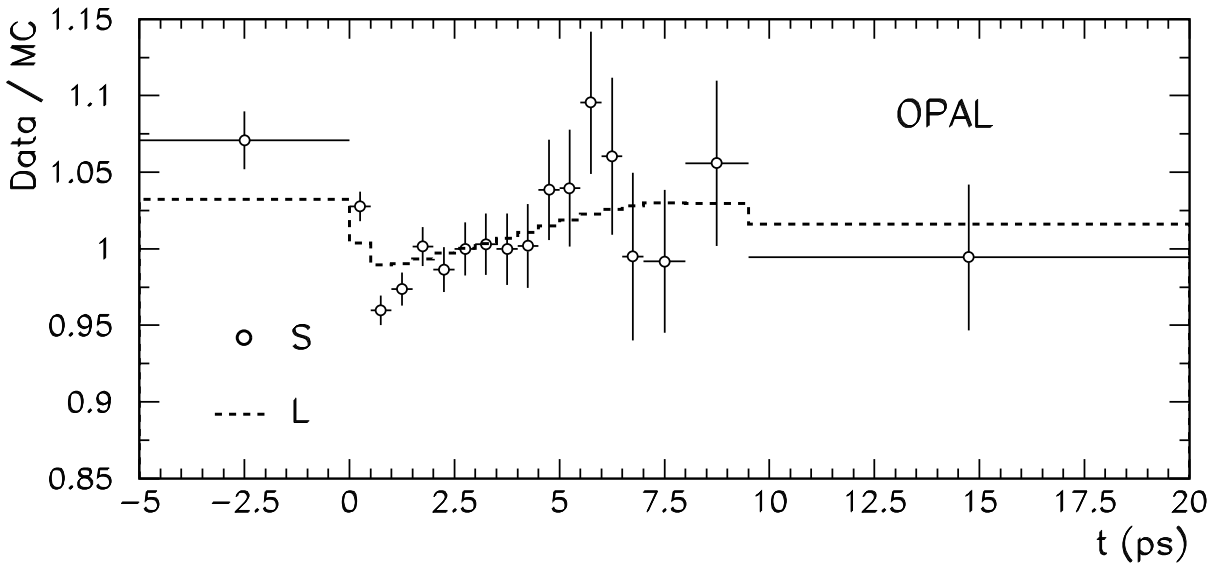

Figure 10: *The distribution of data/Monte Carlo,* $\mathbb{S}(\mathrm{t})$*, for the reconstructed time distributions (points) and the ratio of likelihood predictions,* $\mathbb{L}(\mathrm{t};\tau_\mathrm{b},\vec{\mathrm{a}})$.

Carlo was reweighted to that observed in data. The signal resolution function was parametrised using this new sample of true and reconstructed decay times and the resultant change in the fitted lifetime was 0.002 ps. Secondly, the reconstructed b energy distribution in Monte Carlo was reweighted to correspond to a one standard deviation shift in $\langle \mathrm{x_E} \rangle$ (described in section 3). The change in the fitted lifetime was 0.008 ps. The total systematic error assigned to uncertainties in the b fragmentation is the quadrature sum of the two effects, 0.008 ps.

In order to test systematic effects due to uncertainties in the background, the bias function and also the resolution function, the fitted value of τ_b was studied as the lower cut-off on the reconstructed decay time was increased from -5 ps up to 4 ps. The result of this study is shown in figure 11. The resulting values of τ_b are consistent with the central value across the full time range. However, a systematic error is assigned from the difference between the fitted central value and the value of τ_b with a lower cut-off of 1 ps, added in quadrature with the statistical error on this difference. Both the background and the bias function are thought to contribute a negligible uncertainty to the reconstructed time distribution above 1 ps, as indicated in figures 5 and 7, respectively. The resulting systematic error is determined to be ± 0.015 ps.

This error should partly cover also the uncertainties in the signal resolution function due to uncertainties in the Monte Carlo modelling of the impact parameter resolution for charged tracks, but, to be conservative, a separate estimate of this systematic error was assigned. To investigate this source of uncertainty, the resolution functions were parametrised using the unsmeared Monte Carlo sample. This resulted in a fitted lifetime that was increased by 0.031 ps relative to the central value. This Monte Carlo sample fails to describe tails of impact parameter distributions, as seen in figure 1. One half of the deviation was assigned as a systematic uncertainty. An alternate smearing algorithm [18] gave consistent results.

Studies of different classes of events in the Monte Carlo reveal that the resolution function is different for different charm hadrons produced in the b decay. Specifically, decays yielding a D^+ meson tend to have larger reconstructed times than average, and those yielding Λ_c particles tend to have smaller reconstructed times than average. Previous measurements from OPAL [22]

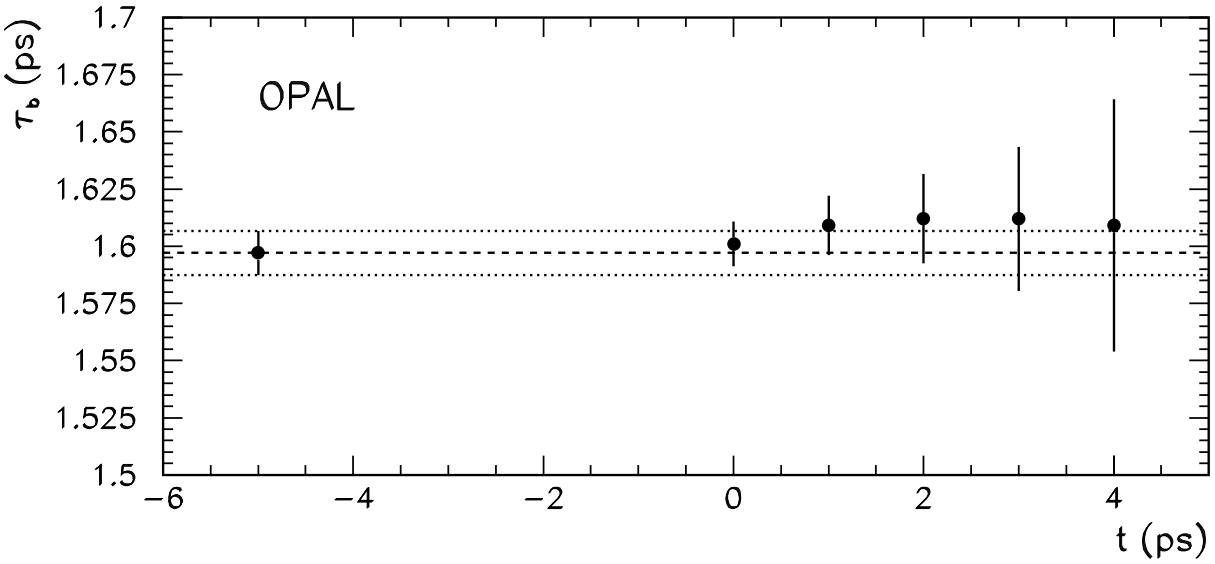

Figure 11: *The value of τ_b from the χ^2 fit for various minimum values of reconstructed decay time, using the $\mathbb{S}/\mathbb{L}$ formalism described in the text. The horizontal band represents the lifetime and error determined using the default time cut-off of −5 ps.*

indicate that the rate of D^+ production per b hadron decay is (18.8±2.3)% and the corresponding rate for Λ_c production is (12.5 ± 3.1)%. In the Monte Carlo simulation these rates were 22.7% and 11.3%, respectively, so the fitted b lifetime was shifted by +0.014 ps to 1.611 ps in order to account for these differences, and systematic errors were assigned to cover the uncertainties in the measured rates. These errors were 0.007 ps for both the D^+ and Λ_c rates. The sensitivity to decays resulting in two charm hadrons, occurring in 15% of b decays in the Monte Carlo, was also investigated. A 5% uncertainty (relative to the number of b decays) on this decay rate would result in an uncertainty of 0.009 ps on τ_b. However, the effect was found to be negligible for reconstructed times larger than 1 ps. No systematic error was assigned for this effect, since it is considered to be covered by the error assigned using a low cut-off of 1 ps on the reconstructed time, as described above.

A lifetime error of ±0.008 ps was assigned due to the uncertainty on the proportion of signal events, ζ. This was estimated using one standard deviation errors on the value of ζ derived from double tagging with corrections from Monte Carlo, $\zeta = 0.956 \pm 0.006$. To include such a systematic error may be double counting, since the background uncertainty is also covered by the comparison with the result for times larger than 1 ps. In addition, to account for possible uncertainties in the composition of the background (predominantly due to c or u, d or s quarks), the background resolution function was reparametrised reducing the contribution from u, d and s quarks by a factor of two. All other parameters in the lifetime fit were left unchanged. A systematic error of ±0.003 ps was assigned to account for the change in fitted lifetime.

Alignment studies indicate that the radial position of the silicon detectors is known to within 50 μm. This could introduce a systematic effect in the determination of the b hadron decay length. The effect is modelled by shifting both layers of silicon detectors coherently and re-determining the decay length. A shift in the mean reconstructed decay time of 0.0045±0.0015 ps was observed and a conservative systematic error of ±0.006 ps was therefore assigned to this

Source of Uncertainty	Correction (ps)	Systematic Error (ps)
b fragmentation		± 0.008
Background and bias correction function		± 0.015
Impact parameter resolution		± 0.016
D^+ production rate	$+0.012$	± 0.007
Λ_c production rate	$+0.002$	± 0.007
Signal proportion		± 0.008
Background composition		± 0.003
Silicon detector alignment		± 0.006
Total	$+0.014$	± 0.027

Table 4: *A summary of the corrections and systematic errors assigned to* τ_b.

Year	Signal Proportion, ζ (%)	τ_b (ps)
1991	94.8 ± 1.3	1.548 ± 0.028
1992	95.3 ± 0.7	1.607 ± 0.016
1993	95.8 ± 0.7	1.598 ± 0.017
1994	95.7 ± 0.6	1.628 ± 0.013
1991–4 (w.a.)	95.6 ± 0.4	1.610 ± 0.010
1991–4 (full)	95.6 ± 0.4	1.611 ± 0.010

Table 5: *The value of the signal proportion,* ζ*, evaluated for each year of data-taking using a double tagging technique. The resulting fitted value of* τ_b *is also shown. The errors indicated on both* ζ *and* τ_b *are purely statistical. The* ζ *and* τ_b *results for 1991–1994 are from an error weighted average of each individual year (w.a.) and a fit to all four years together (full).*

source of uncertainty.

As a cross-check of the overall method, the data set was divided into four years (1991–1994) and each year was fitted separately. Data from 1991 to 1994 made up approximately 8%, 26%, 21% and 45%, respectively, of the total data-set. The value of ζ derived for each year, from the double tagging technique with associated Monte Carlo corrections, is shown in table 5 with the corresponding fitted lifetime.

The error weighted average of individual lifetime results from each year is consistent with the central lifetime result. The χ^2 per degree of freedom between the individual lifetime results and the combined result is 2.9, which corresponds to a probability of 3.5%. If the statistical error on ζ is taken into account for each year, then the χ^2 per degree of freedom is reduced to 2.1, with a probability of 9.4%. When the same test is performed with a low cut-off of 1 ps, the agreement is excellent: $\chi^2 = 0.19$ per degree of freedom. Thus any potential systematic problem would seem to be already covered by the comparison with the result for times greater than 1 ps.

10 Conclusions

Approximately 3.5 million hadronic events recorded by the OPAL detector between 1991 and 1994 have been used to measure τ_b. These events have been used to reconstruct 95 620 b hadron decay times. The b hadron decay time is reconstructed from measurements of the b hadron

decay length and momentum. A fit to the ratio of the reconstructed decay time distributions seen in data and Monte Carlo is used to extract

$$\tau_{\rm b} = 1.611 \pm 0.010\,(\text{stat}) \pm 0.027\,(\text{syst})\ \text{ps}. \tag{28}$$

The largest contributions to the systematic error result from the Monte Carlo modelling of impact parameter resolutions, the bias due to selection criteria and background.

The current world average is $\tau_{\rm b} = 1.549 \pm 0.020$ ps [11]. The result presented in this paper is compatible with this at the level of 1.8 standard deviations, assuming uncorrelated systematic errors, and has a competitive precision. We also note that results have been obtained by the DELPHI and SLD collaborations [3] using inclusively reconstructed secondary vertices. They measure $\tau_{\rm b} = 1.582 \pm 0.011\,(\text{stat}) \pm 0.027\,(\text{syst})$ ps and $\tau_{\rm b} = 1.564 \pm 0.030\,(\text{stat}) \pm 0.036\,(\text{syst})$ ps, respectively, in good agreement with the result presented here.

Acknowledgements

We particularly wish to thank the SL Division for the efficient operation of the LEP accelerator and for their continuing close cooperation with our experimental group. In addition to the support staff at our own institutions we are pleased to acknowledge the
Department of Energy, USA,
National Science Foundation, USA,
Particle Physics and Astronomy Research Council, UK,
Natural Sciences and Engineering Research Council, Canada,
Israel Science Foundation, administered by the Israel Academy of Science and Humanities,
Minerva Gesellschaft,
Japanese Ministry of Education, Science and Culture (the Monbusho) and a grant under the Monbusho International Science Research Program,
German Israeli Bi-national Science Foundation (GIF),
Direction des Sciences de la Matière du Commissariat à l'Energie Atomique, France,
Bundesministerium für Bildung, Wissenschaft, Forschung und Technologie, Germany,
National Research Council of Canada,
Hungarian Foundation for Scientific Research, OTKA T-016660, and OTKA F-015089.

References

[1] L3 Collaboration, O. Adriani *et al.*, Phys. Lett. **B317** (1993) 474;
ALEPH Collaboration, D. Buskulic *et al.*, Phys. Lett. **B369** (1996) 151;
DELPHI Collaboration, P. Abreu *et al.*, Z. Phys. **C63** (1994) 3.

[2] OPAL Collaboration, P.D. Acton *et al.*, Z. Phys. **C60** (1993) 217.

[3] DELPHI Collaboration, P. Abreu *et al.*, Phys. Lett. **B377** (1996) 195;
SLD Collaboration, K. Abe *et al.*, Phys. Rev. Lett. **75** (1995) 3624.

[4] OPAL Collaboration, K. Ahmet *et al.*, Nucl. Instr. Meth. **A305** (1991) 275.

[5] O. Biebel *et al.*, Nucl. Instr. and Meth. **A323** (1992) 169;
M. Hauschild *et al.*, Nucl. Instr. and Meth. **A314** (1992) 74.

[6] P.P. Allport *et al.*, Nucl. Instr. Meth. **A324** (1993) 34.

[7] P.P. Allport *et al.*, Nucl. Instr. Meth. **A346** (1994) 476.

[8] OPAL Collaboration, G. Alexander *et al.*, Z. Phys. **C52** (1991) 175.

[9] T. Sjöstrand, Comp. Phys. Comm. **82** (1994) 74.

[10] OPAL Collaboration, G. Alexander *et al.*, Z. Phys. **C69** (1996) 543.

[11] The Particle Data Group, R.M. Barnett *et al.*, Phys. Rev. **D54** (1996) 1.

[12] C. Peterson, D. Schlatter, I. Schmitt and P. Zerwas, Phys. Rev. **D 27** (1983) 105.

[13] OPAL Collaboration, G. Alexander *et al.*, Phys. Lett. **B364** (1995) 93;
ALEPH Collaboration, D. Buskulic *et al.*, Phys. Lett. **B357** (1995) 699.

[14] J. Allison *et al.*, Nucl. Instr. and Meth. **A317** (1992) 47.

[15] OPAL Collaboration, R. Akers *et al.*, Z. Phys. **C61** (1994) 209.

[16] OPAL Collaboration, R. Akers *et al.*, Z. Phys. **C66** (1995) 19.

[17] OPAL Collaboration, R. Akers *et al.*, Z. Phys. **C68** (1995) 179.
The jet finding parameters ϵ and R were set to 5.0 GeV and 0.65, respectively.

[18] OPAL Collaboration, R. Akers *et al.*, Z. Phys. **C65** (1995) 17.

[19] OPAL Collaboration, R. Akers *et al.*, 'An Update of the Measurement of R_{b} using a Double Tagging Method', to be submitted to Z. Phys. C.

[20] OPAL Collaboration, R. Akers *et al.*, Z. Phys. **C66** (1995) 555.

[21] OPAL Collaboration, R. Akers *et al.*, Z. Phys. **C66** (1995) 19.

[22] OPAL Collaboration, G. Alexander *et al.*, CERN-PPE/96-51, to be published in Z. Phys. C.